Latin American Journal of Solids and Structures
www.lajss.org

Probabilistic analysis of stress intensity factor (SIF) and degree of bending (DoB) in axially loaded tubular K-joints of offshore structures

Abstract

The stress intensity factor (SIF) and the degree of bending (DoB) are among the crucial parameters in evaluating the fatigue reliability of offshore tubular joints based on the fracture mechanics (FM) approach. The value of SIF is a function of the crack size, nominal stress, and two modifying coefficients known as the crack shape factor (Y_c) and geometric factor (Y_g). The value of the DoB is mainly determined by the joint geometry. These three parameters exhibit considerable scatter which calls for greater emphasis in accurate determination of their governing probability distributions. As far as the authors are aware, no comprehensive research has been carried out on the probability distribution of the DoB and geometric and crack shape factors in tubular joints. What has been used so far as the probability distribution of these factors in the FM-based reliability analysis of offshore structures is mainly based on assumptions and limited observations, especially in terms of distribution parameters. In the present paper, results of parametric equations available for the computation of the DoB, Y_c, and Y_g have been used to propose probability distribution models for these parameters in tubular K-joints under balanced axial loads. Based on a parametric study, a set of samples were prepared for the DoB, Y_c, and Y_g; and the density histograms were generated for these samples using Freedman-Diaconis method. Ten different probability density functions (PDFs) were fitted to these histograms. The maximum likelihood (ML) method was used to determine the parameters of fitted distributions. In each case, Kolmogorov-Smirnov test was used to evaluate the goodness of fit. Finally, after substituting the values of estimated parameters for each distribution, a set of fully defined PDFs were proposed for the DoB, crack shape factor (Y_c), and geometric factor (Y_g) in tubular K-joints subjected to balanced axial loads.

Keywords

Tubular K-joint; degree of bending (DoB); stress intensity factor (SIF); geometric factor; crack shape factor; probability density function (PDF); Kolmogorov-Smirnov goodness-of-fit test.

Hamid Ahmadi[a]
Amirreza Ghaffari[b]

[a,b]Faculty of Civil Engineering,
University of Tabriz,
Tabriz 5166616471, Iran

Corresponding author:
[a]h-ahmadi@tabrizu.ac.ir
[b]a.ghaffari.t@gmail.com

http://dx.doi.org/10.1590/1679-78251698

Received 15.11.2014
Accepted 30.05.2015
Available online 07.07.2015

1 INTRODUCTION

Tubular K-joints are frequently adapted in the substructure of offshore jacket-type platforms. Figure 1 shows a tubular K-joint along with the three commonly named positions along the brace/chord intersection: saddle, toe, and heel. Non-dimensional geometrical parameters including α, β, γ, τ, and ζ which are used to easily relate the behavior of a tubular joint to its geometrical characteristics are defined in Figure 1.

Tubular joints are subjected to cyclic loads induced by sea waves and hence they are susceptible to fatigue damage due to the formation and propagation of cracks. Thus, the estimation of the residual life of the cracked joints is crucial. The most commonly used method, to estimate how many cycles a K-joint will sustain before its through-thickness failure, is to refer to an S–N curve (American Petroleum Institute, 2007). When a K-joint is loaded, the hot-spot stress (HSS) range can be obtained through the multiplication of nominal stress range by the stress concentration factor (SCF). Using the S–N curve, the number of cycles can be predicted according to the corresponding HSS range. However, for a K-joint with an initial surface crack, the S–N curve can no longer be applied. In this case, an alternative method to estimate the remaining life of a cracked K-joint is to use fracture mechanics (FM) approach based on the stress intensity factors (SIFs). Moreover, the investigation of a large number of fatigue test results have shown that tubular joints with different geometry or loading type but with similar HSSs often can endure significantly different numbers of cycles before failure (Connolly, 1986). These differences are thought to be attributable to changes in crack growth rate which is dependent on the through-the-thickness stress distribution as well as the HSS. The stress distribution across the wall thickness which is assumed to be a linear combination of membrane and bending stresses can be characterized by the degree of bending (DoB), i.e. the ratio of bending stress to total stress.

Deterministic FM analyses typically produce conservative results, since limiting assumptions are to be made on key input parameters. However, some of the key parameters of the problem, such as the SIF and DoB can exhibit considerable scatter. This highlights the necessity of conducting a reliability analysis in which these parameters can be modeled as random quantities. Reliability against fatigue and fracture failure becomes always important in case of random and cyclic excitation (Mohammadzadeh et al., 2014). The fundamentals of reliability assessment, if properly applied, can provide immense insight into the performance and safety of the structural system. The value of SIF is a function of the crack size, nominal stress, and two modifying coefficients called the geometric factor (Y_g) and crack shape factor (Y_c). The value of the DoB is mainly determined by the joint geometry. These three parameters exhibit considerable scatter which calls for greater emphasis in accurate determination of their governing probability distributions. As far as the authors are aware, despite the considerable research work accomplished on the deterministic study of SCFs and SIFs in tubular joints (e.g. Bowness and Lee (1998), Lee et al. (2005), Shao and Lie (2005) and Shao (2006) for SIFs; and Wordsworth and Smedley (1978), Efthymiou (1988), Hellier et al. (1990), Morgan and Lee (1998a), Chang and Dover (1999), Shao (2007), Shao et al. (2009), Lotfollahi-Yaghin and Ahmadi (2010), Ahmadi et al. (2011), Lotfollahi-Yaghin and Ahmadi (2011), Ahmadi and Lotfollahi-Yaghin (2012), and Ahmadi et al. (2013) for SCFs, among others), no comprehensive research has been carried out on the probability distribution of the DoB and geometric and crack shape factors in tubular joints. What has been used so far as the probability distribution

of these parameters in the FM-based reliability analysis of offshore structures is mainly based on assumptions and limited observations, especially in terms of distribution parameters.

In the present paper, results of parametric equations available for the computation of the DoB, Y_g, and Y_c have been used to propose probability distribution models for these parameters in tubular K-joints under balanced axial loads. Based on a parametric study, a set of samples were prepared for the DoB, Y_g, and Y_c; and the density histograms were generated for these samples using Freedman-Diaconis method. Ten different probability density functions (PDFs) were fitted to these histograms. The maximum likelihood (ML) method was used to determine the parameters of fitted distributions; and in each case, Kolmogorov-Smirnov test was utilized to evaluate the goodness of fit. Finally, the best-fitted distributions were selected and are introduced in the present paper. The proposed PDFs can be adapted in the FM-based fatigue reliability analysis of tubular K-joints commonly found in offshore jacket structures.

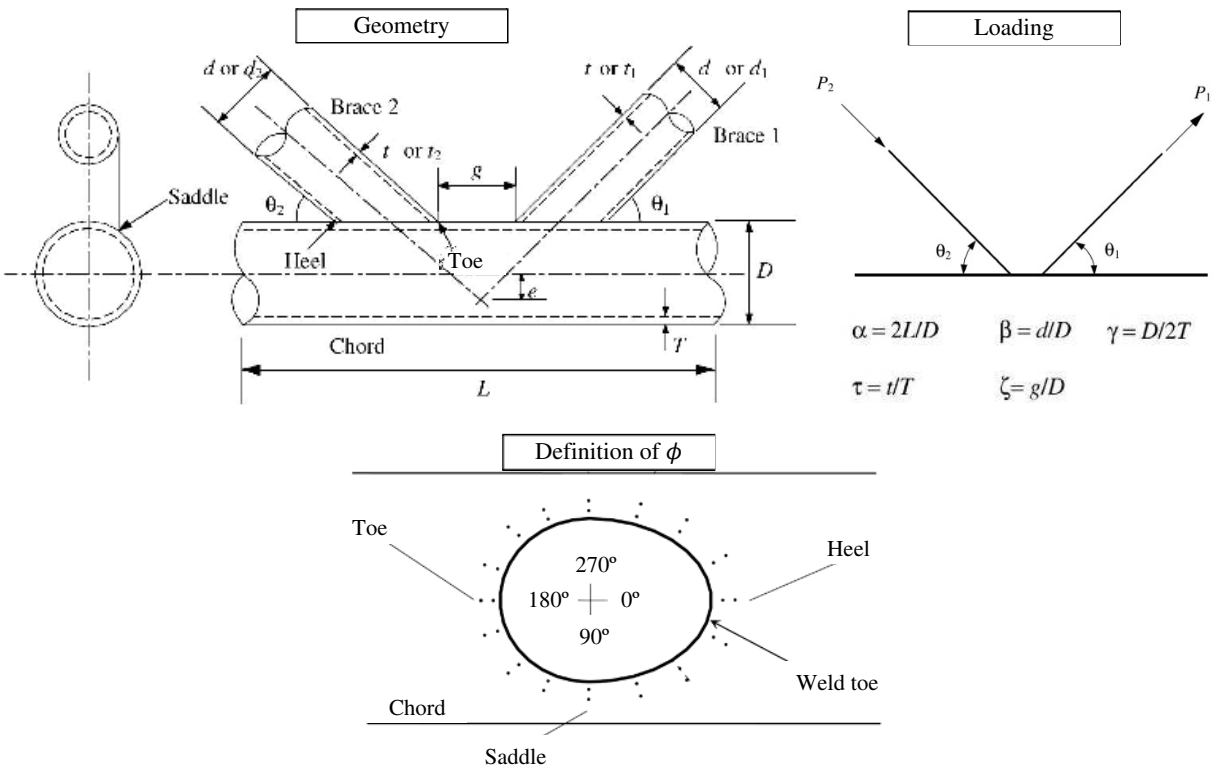


Figure 1: Geometrical notation for an axially loaded tubular K-joint.

2 THE FORMULATION OF SIF IN TUBULAR K-JOINTS SUBJECTED TO BALANCED AXIAL LOADS

The SIF can be calculated as follows:

$$\text{SIF} = Y_g Y_c \sigma_{\text{nom}} \sqrt{\pi a} \tag{1}$$

where σ_{nom} is the nominal stress, a is the crack size, Y_g is the geometric factor, and Y_c is the crack shape factor. Both Y_g and Y_c are dimensionless quantities.

In a tubular K-joint subjected to balanced axial loads, the nominal stress is computed as:

$$\sigma_{\text{nom}} = \frac{4P}{\pi\left[d^2 - \left(d - 2t\right)^2\right]} \tag{2}$$

where P, d, and t are defined in Figure 1.

Geometric factor for a tubular K-joint subjected to balanced axial loads can be calculated using following equation (Shao and Lie, 2005):

$$Y_g = \left(\frac{\gamma}{12}\right)^{0.43577}\left(1.557\tau + 0.131486\right)\left(0.42659\theta_1 + 0.8275\right)\left(-0.42414\theta_2 + 1.489\right)\beta^{-0.219366} \tag{3}$$

where θ_1 and θ_2 should be inserted in radians.

The expression for crack shape factor is (Shao and Lie, 2005):

$$Y_c = \left(\frac{a}{T}\right)^{-0.141}\left[\left(\frac{c}{a}\right)/5\right]^{0.36} \tag{4}$$

where T is the thickness of the chord; and a and c are crack dimensions illustrated in Figure 2.

The validity ranges for the application of Eqs. (3) and (4) are as follows:

$$\begin{aligned} &t_1 = t_2 = t;\ d_1 = d_2 = d \\ &\gamma = D/2T \in \left[12,\ 30\right]\ ;\ \beta = d/D \in \left[0.3, 0.6\right]\ ;\ \tau = t/T \in \left[0.25,\ 1.0\right] \\ &c/a \in \left[5,\ 8\right]\ ;\ a/T \in \left[0.1,\ 0.7\right] \\ &\theta_1 \in \left[30^\circ,\ 60^\circ\right]\ ;\ \theta_2 \in \left[30^\circ,\ 60^\circ\right]\ ;\ e = 0 \end{aligned} \tag{5}$$

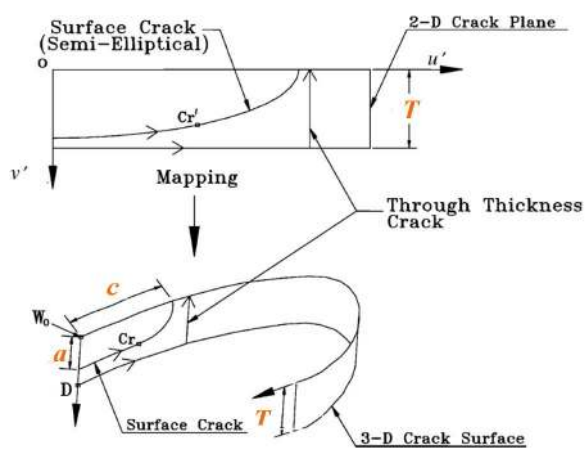


Figure 2: Crack dimensions a and c through the chord thickness T.

3 THE FORMULATION OF DoB IN AXIALLY LOADED TUBULAR K-JOINTS

As mentioned earlier, the degree of bending (DoB) is the ratio of bending stress over total stress expressed as:

$$\mathrm{DoB} = \frac{\sigma_B}{\sigma_T} = \frac{\sigma_B}{\sigma_B + \sigma_M} \tag{6}$$

where σ_B is the bending stress component, σ_T is the total stress on the outer tube surface, and σ_M is the membrane stress component (Figure 3).

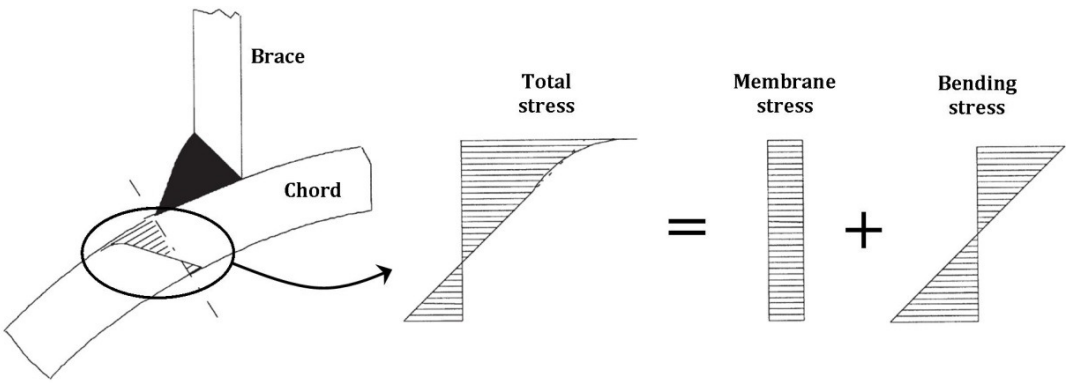


Figure 3: Through-the-thickness stress distribution in a tubular joint.

Morgan and Lee (1998b) proposed a set of equations for the calculation of DoBs in tubular K-joints subjected to balanced axial loads (Eqs. (7)−(12)). In Eq. (7), $\mathrm{DoB_{ch}}$ stands for the DoB at the position of the maximum SCF. In Eqs. (8)−(12), $\mathrm{DoB_{ch0}}$, $\mathrm{DoB_{ch45}}$, $\mathrm{DoB_{ch90}}$, $\mathrm{DoB_{ch135}}$, and $\mathrm{DoB_{ch180}}$ denote the DoB on the chord at $\theta = 0^\circ$, 45°, 90°, 135°, and 180°, respectively; where θ is the polar angle around the weld toe shown in Figure 1.

$$\begin{aligned}\mathrm{DoB_{Ch}} &= \tau^{0.017}\gamma^{0.092}(1.34 + 0.01\beta + 0.228\beta^2)\sin^{0.166}\theta \\ &[0.504 - 0.547\beta^{1.97}\tau^{-0.921}\arctan(0.194\zeta)]\left(\frac{\theta_{\max}}{\theta}\right)^{-0.077}\left(\frac{\theta_{\min}}{\theta}\right)^{0.042}\end{aligned} \tag{7}$$

$$\begin{aligned}\mathrm{DoB_{Ch0}} &= 0.135\gamma^{-0.22}(3.954 - 2.765\beta + 2.023\beta^2) \\ &\sin^{-0.635}\theta\tau^{0.007}[2.987 - 14.751\beta^{-0.444}\arctan(0.013\zeta)]\,f(\alpha)\end{aligned} \tag{8}$$

$$\begin{aligned}\mathrm{DoB_{Ch45}} &= 0.467\gamma^{0.03}(1.021 + 0.592\beta - 0.325\beta^2) \\ &\sin^{-0.193}\theta\tau^{0.025}[1.382 - 1.39\beta^{0.661}\arctan(0.063\zeta)]\end{aligned} \tag{9}$$

$$\begin{aligned}\mathrm{DoB_{Ch90}} &= 1.704\gamma^{-1.052}(-2.222 - 3.466\beta + 15.522\beta^2) \\ &\sin^{13.809}\theta\tau^{3.016}[4.325 - 24.963\beta^{0.45}\arctan(1.605\zeta)] + [\beta^{0.117}\gamma^{0.02}(0.027\tau + 0.892)\theta^{-0.128}]\end{aligned} \tag{10}$$

$$\begin{aligned}
&\mathrm{DoB}_{\mathrm{Ch135}} = 0.359\gamma^{0.044}(1.797 + 0.251\beta - 0.015\beta^2)\sin^{-0.281}\theta \\
&\tau^{0.02}[0.81 + 0.13\beta^{-1.205}\arctan(0.244\zeta)] \\
&\left(\frac{\theta_{\max}}{\theta}\right)^{0.03}\left(\frac{\theta_{\min}}{\theta}\right)^{-0.13}\left(\frac{\beta}{\beta_{\min}}\right)^{[39.582(\beta_{\min}/\beta_{\max})-23.887]} f(\beta)
\end{aligned} \tag{11}$$

$$f(\beta) = \begin{cases} 1.395\theta^{0.142}\tau^{-0.201} & \text{for cases where } \beta = 1,\ \theta < 60 \text{ and } \theta_{\max} = \theta_{\min} \\ 1 & \text{for all other cases} \end{cases}$$

$$\begin{aligned}
&\mathrm{DoB}_{\mathrm{Ch180}} = 0.795\gamma^{-0.002}(0.755 + 0.266\beta - 0.083\beta^2) \\
&\sin^{0.215}\theta\tau^{0.021}[1.453 - 0.479\beta^{0.002}\arctan(1.342\zeta)]
\end{aligned} \tag{12}$$

The validity ranges for the application of Eqs. (7)−(12) are as follows:

$$\begin{aligned}
&t_1 = t_2 = t\ ;\ d_1 = d_2 = d\ ;\ \theta_1 = \theta_2 = \theta \\
&\gamma = D/2T \in [10,\ 40]\ ;\ \beta = d/D \in [0.3,\ 1]\ ;\ \tau = t/T \in [0.2,\ 1] \\
&\theta \in [30^\circ,\ 90^\circ]\ ;\ \zeta \in [0.1,\ 0.8]\ ;\ \alpha \in [6,\ 40]
\end{aligned} \tag{13}$$

4 PREPARATION OF THE SAMPLE DATABASE

Using MATLAB, a computer code was developed by the authors to generate eight samples for the geometric and crack shape factors, $\mathrm{DoB_{ch}}$, $\mathrm{DoB_{ch0}}$, $\mathrm{DoB_{ch45}}$, $\mathrm{DoB_{ch90}}$, $\mathrm{DoB_{ch135}}$, and $\mathrm{DoB_{ch180}}$ based on Eqs. (3)−(5) and (7)−(13). Values of the size (n), mean (μ), standard deviation (σ), coefficient of skewness (a_3), and coefficient of kurtosis (a_4) for these samples are listed in Tables 1 and 2.

According to Table 1, the value of a_3 for both Y_c and Y_g samples is positive meaning that in both cases, the distribution is expected to have a longer tail on the right, which is toward increasing values, than on the left. Moreover, in both Y_c and Y_g samples, the value of a_4 is smaller than three which means that, in both cases, the probability distribution is expected to be mild-peak (platykurtic).

As can be seen in Table 2, the value of a_3 for $\mathrm{DoB_{ch}}$, $\mathrm{DoB_{ch0}}$, $\mathrm{DoB_{ch45}}$, $\mathrm{DoB_{ch135}}$, and $\mathrm{DoB_{ch180}}$ samples is positive meaning that in these cases, the distribution is expected to have a longer tail on the right, which is toward increasing values, than on the left. However, the $\mathrm{DoB_{ch90}}$ sample has a negative a_3 value which means that its distribution is expected to have a longer tail on the left. Moreover, in $\mathrm{DoB_{ch}}$, $\mathrm{DoB_{ch0}}$, $\mathrm{DoB_{ch45}}$, $\mathrm{DoB_{ch135}}$, and $\mathrm{DoB_{ch180}}$ samples, the value of a_4 is smaller than three which means that, in these cases, the probability distribution is expected to be mild-peak (platykurtic). On the contrary, in $\mathrm{DoB_{ch90}}$ sample, the value of a_4 is greater than three meaning that, in this case, the probability distribution is expected to be sharp-peak (Leptokurtic).

Statistical measure	Value	
	Y_c sample	Y_g sample
n	400	32
μ	4.2347	2.2017
σ	0.6859	1.3384
a_3	0.2851	0.5331
a_4	2.4820	1.9964

Table 1: Values of statistical measures for Y_c and Y_g samples.

Statistical measure	Sample					
	DoB_{ch}	DoB_{ch0}	DoB_{ch45}	DoB_{ch90}	DoB_{ch135}	DoB_{ch180}
n	64	64	729	729	729	729
μ	1.2243	0.9937	0.7973	0.4765	0.2856	0.7904
σ	0.5705	0.2942	0.0707	2.3265	0.4054	0.1098
a_3	0.5538	0.5782	0.0758	-8.3512	0.7266	0.2712
a_4	1.8080	2.6714	2.3867	85.5309	1.5559	2.3190

Table 2: Values of statistical measures for the DoB samples.

5 GENERATION OF THE DENSITY HISTOGRAM USING FREEDMAN-DIACONIS PROCEDURE

For generating a density histogram, the range (R) should be divided into a number of classes/cells/bins. The number of occurrences in each class is counted and tabulated. These are called frequencies. Then, the relative frequency of each class can be obtained through dividing its frequency by the sample size. Afterwards, the density is calculated for each class through dividing the relative frequency by the class width. The width of classes is usually made equal to facilitate interpretation.

Care should be exercised in the choice of the number of classes (n_c). Too few will cause an omission of some important features of the data; too many will not give a clear overall picture because there may be high fluctuations in the frequencies. In the present research, Freedman-Diaconis rule was adapted to determine the number of classes:

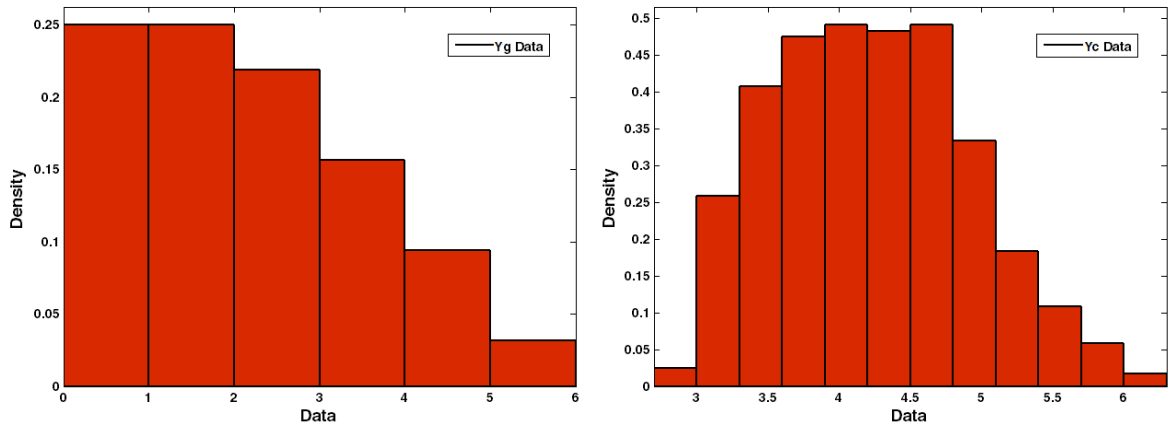
$$n_c = \frac{R\left(n^{1/3}\right)}{2\left(\mathrm{IQR}\right)} \tag{14}$$

where R is the range of sample data, n is the sample size, and IQR is the interquartile range calculated as follows:

$$\mathrm{IQR} = Q_3 - Q_1 \tag{15}$$

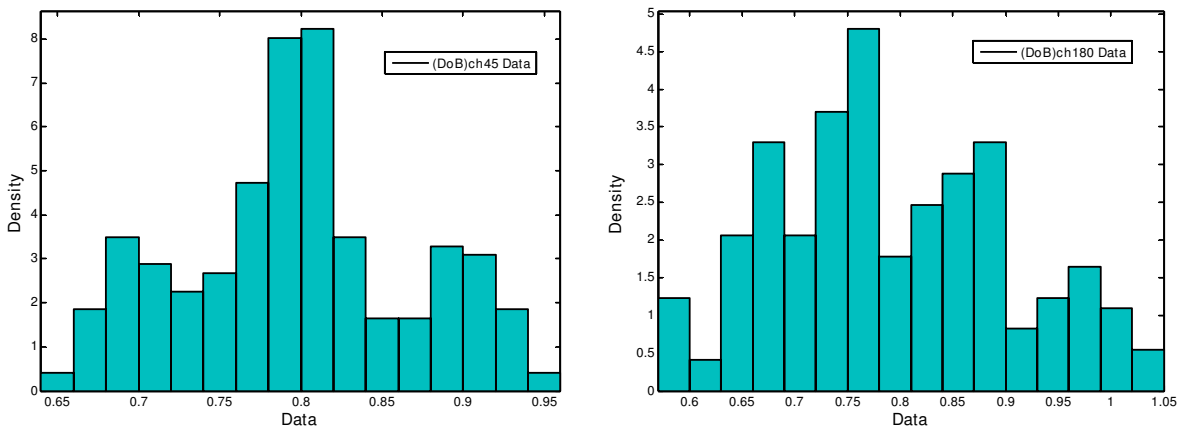
where Q_1 is the lower quartile which is the median of the lower half of the data; and likewise, Q_3 is the upper quartile that is the median of the upper half of the data.

For example, density histograms of geometric and crack shape factors are shown in Figure 4; and histograms of DoB_{ch45} and DoB_{ch180} samples are depicted in Figure 5. As it was expected from values of a_3 and a_4 (Tables 1 and 2), all histograms are platykurtic; and in all of them, the right tail is longer than the left one.



(a) (b)

Figure 4: Density histogram of sample data: (a) Geometric factor Y_g, (b) Crack shape factor Y_c.



(a) (b)

Figure 5: Density histograms: (a) DoB_{ch45} sample, (b) DoB_{ch180} sample.

6 PDF FITTING AND THE ESTIMATION OF PARAMETERS BASED ON ML METHOD

In order to investigate the degree of fitting of various distributions to the sample data, ten different PDFs were fitted to the generated histograms. For example, PDFs fitted to density histograms of Y_c, Y_g, DoB_{ch45}, and DoB_{ch180} samples are shown in Figures 6 and 7. It should be noted that the fitted distributions were completely-specified theoretical PDFs.

In each case, distribution parameters were estimated using the maximum likelihood (ML) method. Results are given in Tables 3 and 4. The ML procedure is an alternative to the method of

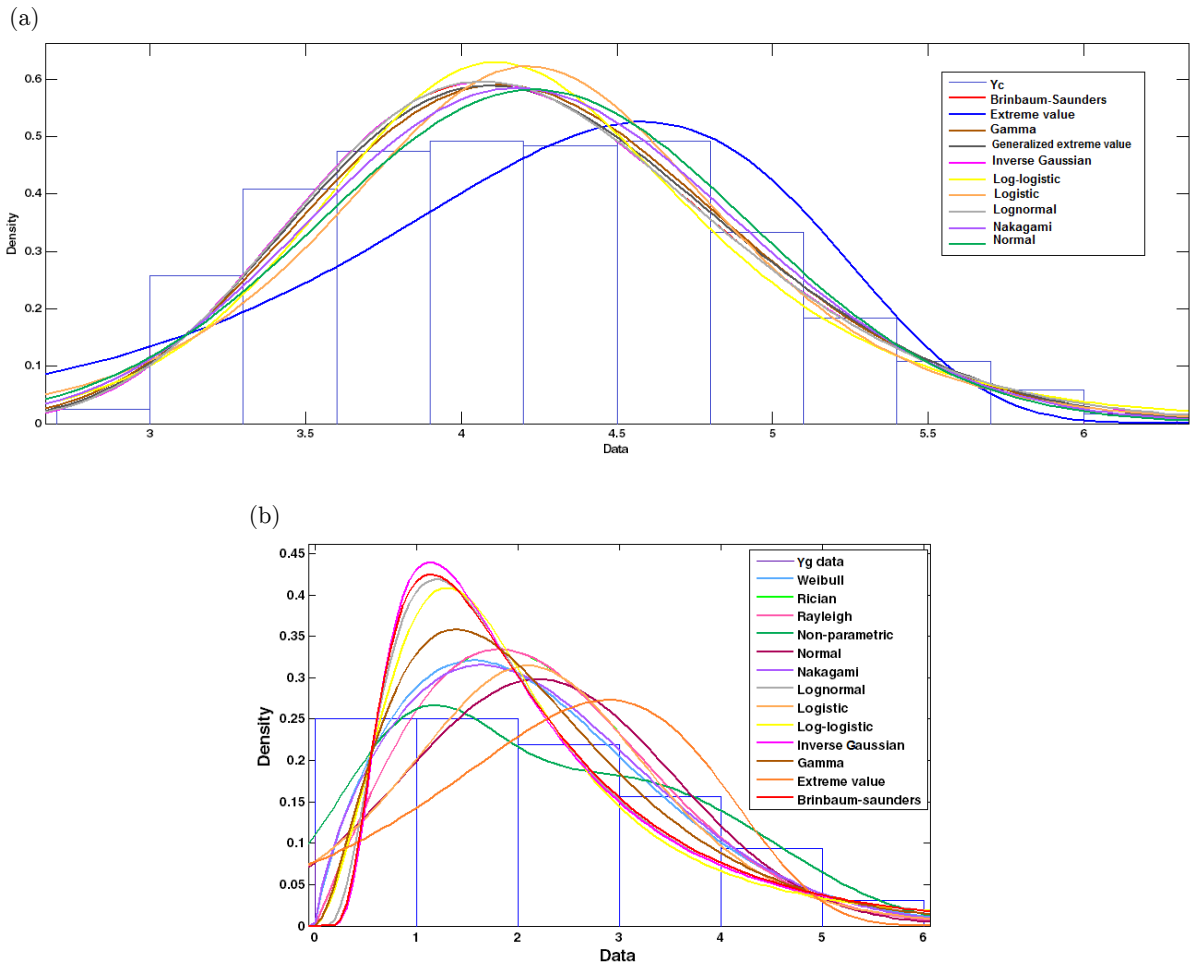


Figure 6: PDFs fitted to the density histogram of sample data: (a) Crack shape factor Y_c, (b) Geometric factor Y_g.

moments. As a means of finding an estimator, statisticians often give it preference. For a random variable X with a known PDF, $f_X(x)$, and observed values x_1, x_2, . . . , x_n, in a random sample of size n, the likelihood function of θ, where θ represents the vector of unknown parameters, is defined as:

$$L(\theta) = \prod_{i=1}^{n} f_X(x_i \mid \theta) \tag{16}$$

The objective is to maximize $L(\theta)$ for the given data set. This is easily done by taking m partial derivatives of $L(\theta)$, where m is the number of parameters, and equating them to zero. We then find the maximum likelihood estimators (MLEs) of the parameter set θ from the solutions of the equations. In this way the greatest probability is given to the observed set of events, provided that we know the true form of the probability distribution.

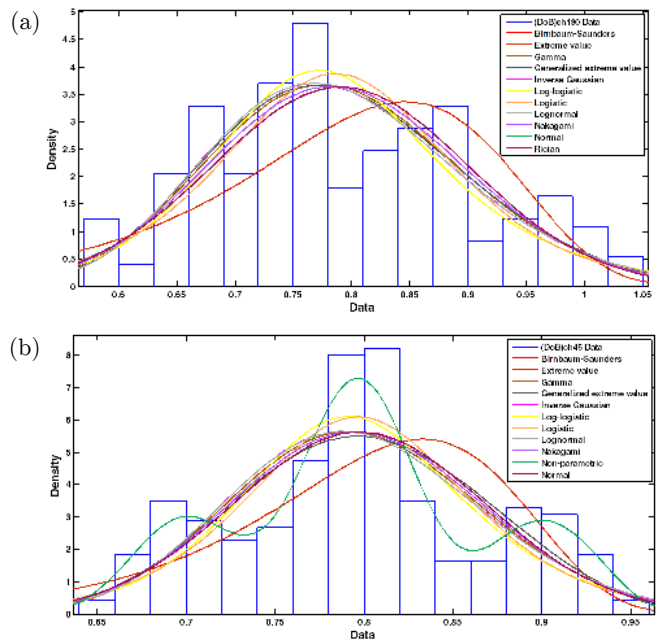


Figure 7: PDF fitted to the density histograms: (a) DoB_{ch45} sample, (b) DoB_{ch180} sample.

Fitted PDF		Estimated parameters	
		Crack shape factor (Y_c) sample	Geometric factor (Y_g) sample
Birnbaum-Saunders	β	4.17957	1.81261
	γ	0.16243	0.655245
Extreme value	μ	4.58519	2.88914
	σ	0.700136	1.34837
Gamma	a	38.39	2.72621
	b	0.110308	0.807614
Generalized extreme value	k	-0.183782	
	σ	0.635822	---
	μ	3.96276	
Inverse Gaussian	μ	4.23471	2.20173
	λ	159.455	4.63102
Log-logistic	β	1.43185	0.594767
	a	0.0956718	0.396898
Logistic	β	4.21602	2.09946
	a	0.401737	0.7954
Lognormal	μ	1.43023	0.594767
	σ	0.162227	0.648587
Nakagami	μ	9.78083	0.847615
	Ω	18.402	6.58296
Normal (Gaussian)	μ	4.23471	2.20173
	σ	0.685854	1.33841
Weibull	a	---	2.48872
	b		1.77255

Table 3: Estimated parameters of PDFs fitted to the density histograms of Y_c and Y_g samples.

Fitted PDF	Parameters	Estimated values					
		DoB_{ch}	DoB_{ch0}	DoB_{ch45}	DoB_{ch90}	DoB_{ch135}	DoB_{ch180}
Birnbaum-Saunders	β	1.10323	0.952592	1.10323			0.782877
	γ	0.468852	0.293792	0.468852			0.138833
Extreme Value	μ	1.52026	1.14692	1.52026			0.846555
	σ	0.570069	0.313862	0.570069			0.109227
Gamma	a	4.8647	11.9476	4.8647			52.2789
	b	0.251668	0.0831714	0.251668			0.0151193
Generalized Extreme Value	k	0.256425	-0.0379108	0.256425			-0.203823
	σ	0.374963	0.240826	0.374963			0.10245
	μ	0.90638	0.861266	0.90638			0.747919
Inverse Gaussian	μ	1.22429	0.993698	1.22429			0.790422
	λ	5.27933	11.2694	5.27933	---	---	40.8117
Log-logistic	β	0.077527	-0.0499401	0.077527			-0.245578
	α	0.280926	0.172563	0.280926			0.0816333
Logistic	β	1.16748	0.973626	1.16748			0.786245
	α	0.342878	0.169379	0.342878			0.0644169
Lognormal	μ	0.0960735	-0.0487548	0.0960735			-0.244782
	σ	0.465141	0.293833	0.465141			0.138674
Nakagami	μ	1.3734	3.13911	1.3734			13.2329
	Ω	1.8193	1.07266	1.8193			0.636797
Normal (Gaussian)	μ	1.22429	0.993698	1.22429			0.790422
	σ	0.570522	0.294248	0.570522			0.109754

Table 4: Estimated parameters of PDFs fitted to the density histograms of DoB samples.

7 EVALUATION OF THE GOODNESS OF FIT USING KOLMOGOROV-SMIRNOV TEST

The Kolmogorov-Smirnov goodness-of-fit test is a nonparametric test based on the cumulative distribution function (CDF) of a continuous variable. It is not applicable to discrete variables. The test statistic, in a two-sided test, is the maximum absolute difference (that is, usually the vertical distance) between the empirical and hypothetical CDFs. For a continuous variate X, let $x_{(1)}$, $x_{(1)}$, ... , $x_{(n)}$ represent the order statistics of a sample of the size n, that is, the values arranged in increasing order. The empirical or sample distribution function $F_n\left(x\right)$ is a step function. This gives the proportion of values not exceeding x and is defined as:

$$F_n\left(x\right)=\begin{cases}0, & \text{For } x<x_{(1)}\\ k/n, & \text{For } x_{(k)}\le x<x_{(k+1)}\ ,\ \ k=1,\ 2,\ ...,\ n-1\\ 1, & \text{For } x\ge x_{(n)}\end{cases} \tag{17}$$

Empirical distribution functions for the Y_c, Y_g, DoB_{ch}, DoB_{ch0}, DoB_{ch45}, and DoB_{ch180} samples have been shown in Figures 8 and 9.

Let $F_0\left(x\right)$ denote a completely specified theoretical continuous CDF. The null hypothesis H_0 is that the true CDF of X is the same as $F_0\left(x\right)$. That is, under the null hypothesis:

$$\lim_{n\to\infty}\Pr\left[F_n(x)=F_0(x)\right]=1 \tag{18}$$

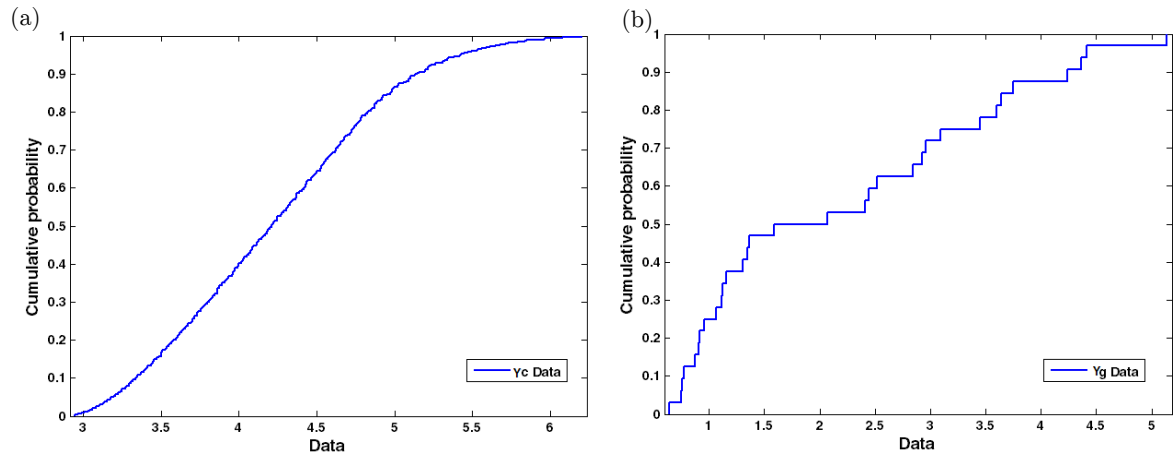


Figure 8: Empirical cumulative distribution functions of sample data:
(a) Crack shape factor Y_c, (b) Geometric factor Y_g.

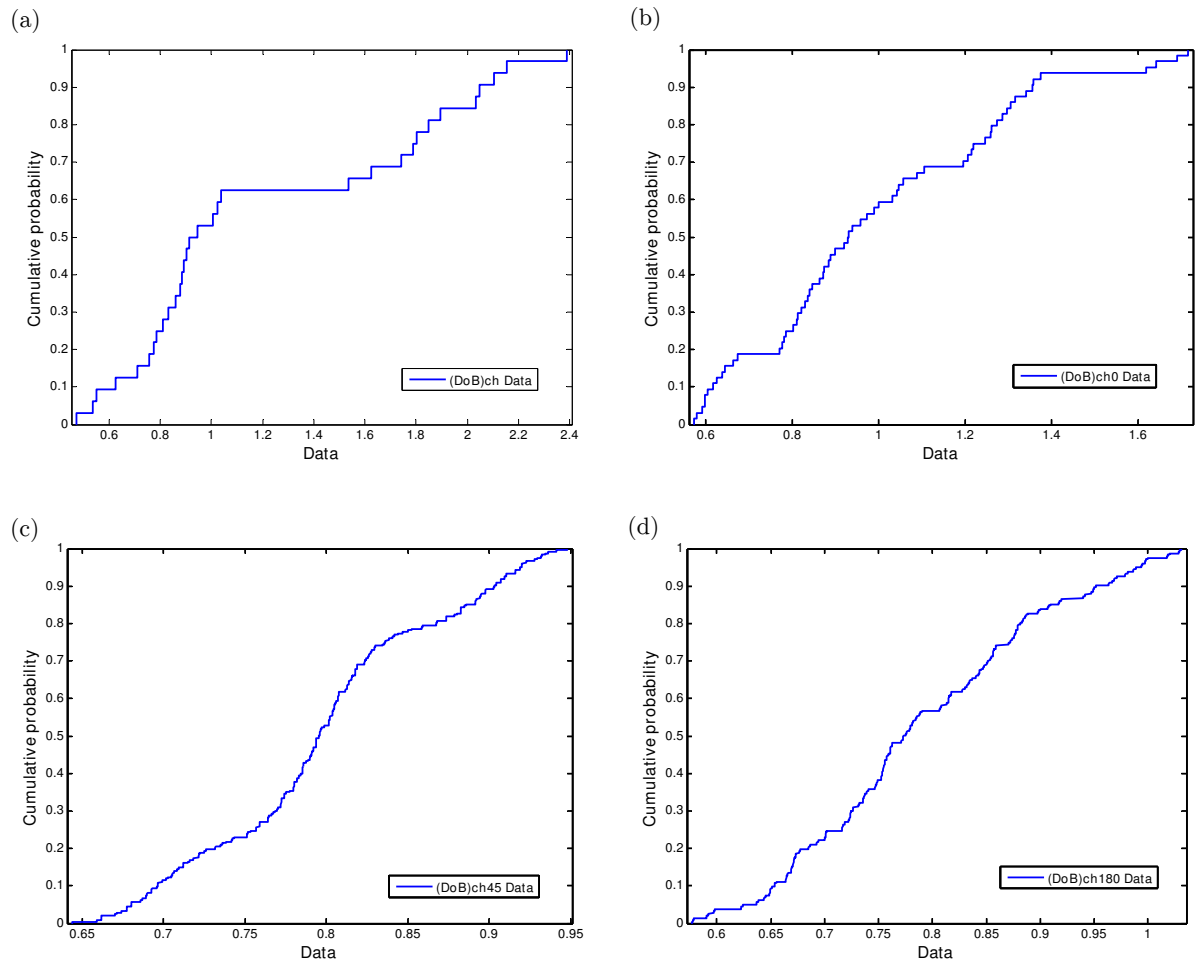


Figure 9: Empirical distribution functions:
(a) DoB_{ch} sample, (b) DoB_{ch0} sample, (c) DoB_{ch45} sample, (d) DoB_{ch180} sample.

The test criterion is the maximum absolute difference between $F_n(x)$ and $F_0(x)$, formally defined as:

$$D_n = \sup_x \left| F_n(x) - F_0(x) \right| \tag{19}$$

Theoretical continuous CDFs fitted to the empirical distribution functions of the Y_c, Y_g, DoB_{ch}, DoB_{ch0}, DoB_{ch45}, and DoB_{ch180} samples have been shown in Figures 10 and 11.

A large value of this statistic (D_n) indicates a poor fit. So critical values should be known. The critical values $D_{n,\alpha}$ for large samples, say $n > 35$, are $(1.3581/\sqrt{n})$ and $(1.6276/\sqrt{n})$ for $a = 0.05$ and 0.01, respectively (Kottegoda and Rosso, 2008).

Results of Kolmogorov-Smirnov test for Y_c, Y_g, DoB_{ch}, DoB_{ch0}, DoB_{ch45}, and DoB_{ch180} sample data are given in Tables 5–10, respectively. It should be noted that, according to the results of Kolmogorov-Smirnov test, none of considered continuous CDFs was acceptably fitted to the DoB_{ch90} and DoB_{ch135} samples. Hence, no table is provided here for these two samples.

It is evident in Tables 5 and 6 that Gamma and Birnbaum-Saunders distributions have the smallest values of test statistic for Y_c and Y_g sample data, respectively. Hence, it can be concluded that Gamma and Birnbaum-Saunders distributions are the best probability models for the crack shape factor (Y_c) and geometric factor (Y_g) in tubular K-joints under balanced axial loads, respectively.

According to Tables 7–10, that Generalized Extreme Value, Gamma, Log-logistic, and Birnbaum-Saunders distributions have the smallest values of test statistic for DoB_{ch}, DoB_{ch0}, DoB_{ch45}, and DoB_{ch180} samples, respectively. Hence, it can be concluded that Generalized Extreme Value, Gamma, Log-logistic, and Birnbaum-Saunders distributions are the best probability models for DoB_{ch}, DoB_{ch0}, DoB_{ch45}, and DoB_{ch180} in axially loaded tubular K-joints, respectively.

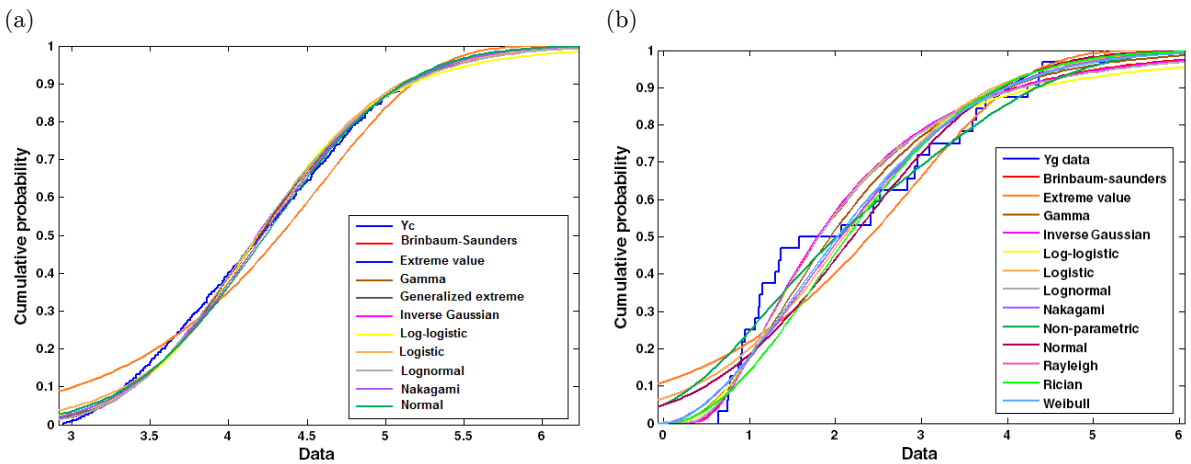


Figure 10: Theoretical continuous CDFs fitted to the empirical distribution function of sample data: (a) Crack shape factor Y_c, (b) Geometric factor Y_g.

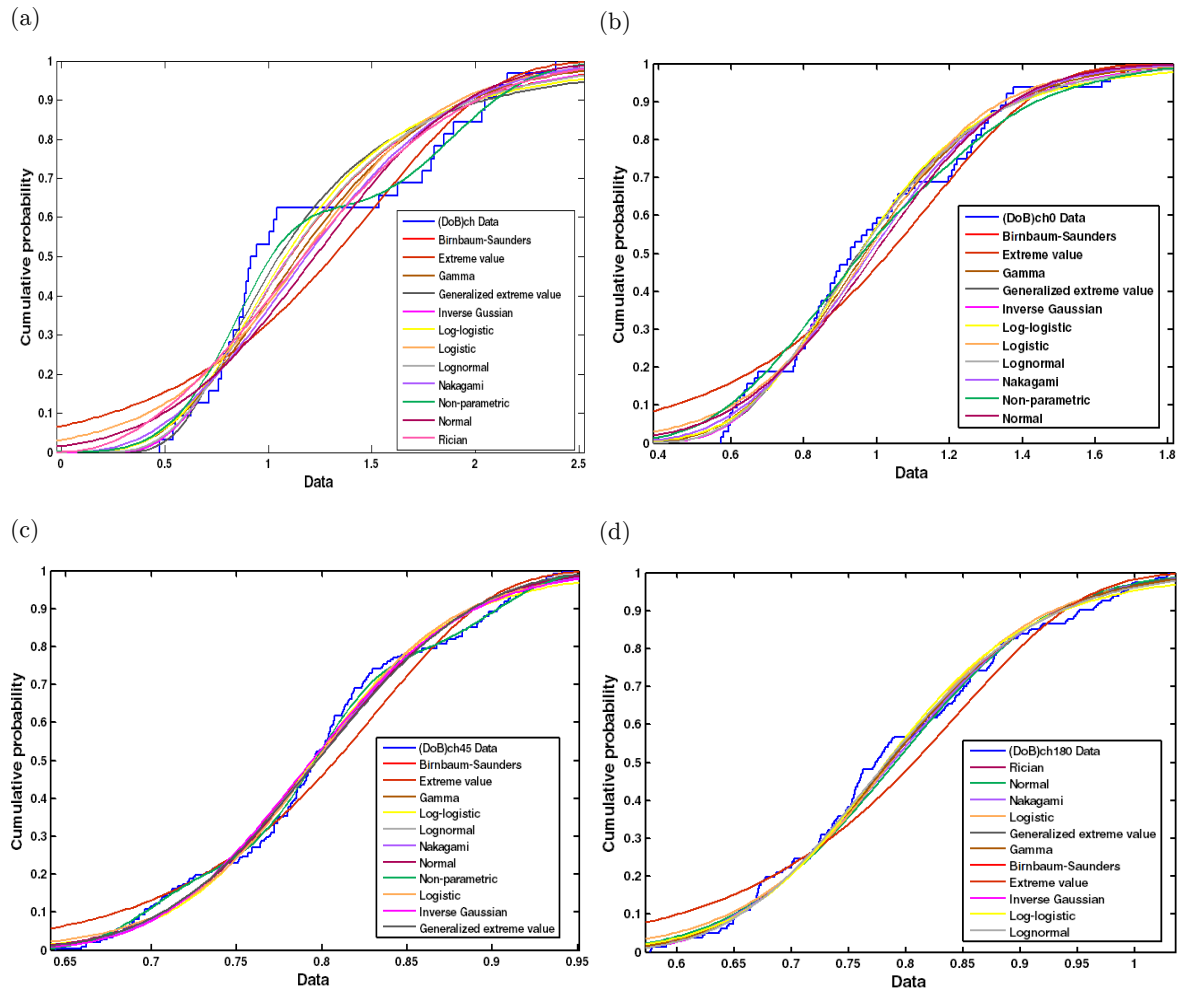


Figure 11: Theoretical CDFs fitted to the empirical distribution functions: (a) DoB_{ch} sample, (b) DoB_{ch0} sample, (c) DoB_{ch45} sample, (d) DoB_{ch180} sample.

Fitted distribution	Test statistic	Critical value		Test result	
		$\alpha = 0.05$	$\alpha = 0.01$	$\alpha = 0.05$	$\alpha = 0.01$
Birnbaum-Saunders	0.0410	0.0675	0.0809	Accept	Accept
Extreme Value	0.0927			Reject	Reject
Gamma	0.0355			Accept	Accept
Generalized Extreme Value	0.0365			Accept	Accept
Inverse Gaussian	0.0411			Accept	Accept
Log-logistic	0.0461			Accept	Accept
Logistic	0.0423			Accept	Accept
Lognormal	0.0411			Accept	Accept
Nakagami	0.0375			Accept	Accept
Normal (Gaussian)	0.0420			Accept	Accept

Table 5: Results of Kolmogorov-Smirnov goodness-of-fit test for Y_c sample data.

Fitted distribution	Test statistic	Critical value		Test result	
		$\alpha = 0.05$	$\alpha = 0.01$	$\alpha = 0.05$	$\alpha = 0.01$
Birnbaum-Saunders	0.1433	0.2343	0.2809	Accept	Accept
Extreme Value	0.1904				
Gamma	0.1695				
Weibull	0.1776				
Inverse Gaussian	0.1451				
Log-logistic	0.1446				
Logistic	0.1810				
Lognormal	0.1438				
Nakagami	0.1854				
Normal (Gaussian)	0.2001				

Table 6: Results of Kolmogorov-Smirnov goodness-of-fit test for Y_g sample data.

Fitted distribution	Test statistic	Critical value		Test result	
		$\alpha = 0.05$	$\alpha = 0.01$	$\alpha = 0.05$	$\alpha = 0.01$
Birnbaum-Saunders	0.1751	0.1669	0.2003	Reject	Accept
Extreme Value	0.2750			Reject	Reject
Gamma	0.2029			Reject	Reject
Generalized Extreme Value	0.1550			Accept	Accept
Inverse Gaussian	0.1718			Reject	Accept
Log-logistic	0.1590			Accept	Accept
Logistic	0.2168			Reject	Reject
Lognormal	0.1736			Reject	Accept
Nakagami	0.2288			Reject	Reject
Normal (Gaussian)	0.2516			Reject	Reject

Table 7: Results of Kolmogorov-Smirnov goodness-of-fit test for $\mathrm{DoB_{ch}}$ simple.

8 PROPOSED PROBABILITY MODELS

Based on the results of Kolmogorov-Smirnov goodness-of-fit test, Gamma and Birnbaum-Saunders distributions are the best probability models for Y_c and Y_g, respectively (Tables 5 and 6). Moreover, Based on the results of Kolmogorov-Smirnov goodness-of-fit test (Tables 7−10), Generalized Extreme Value, Gamma, Log-logistic, and Birnbaum-Saunders distributions are the best probability models for $\mathrm{DoB_{ch}}$, $\mathrm{DoB_{ch0}}$, $\mathrm{DoB_{ch45}}$, and $\mathrm{DoB_{ch180}}$, respectively. The PDFs of these distributions are given by the following equations:

$$f_X(x) = \frac{1}{b^a \Gamma(a)} x^{a-1} e^{-x/b} \quad \text{Gamma distribution} \tag{20}$$

$$f_X(x) = \frac{1}{\sqrt{2\pi}} \exp\left\{ -\frac{\left(\sqrt{x\,/\,\beta} - \sqrt{\beta\,/\,x}\right)^2}{2\gamma^2} \right\} \left(\frac{\sqrt{x\,/\,\beta} + \sqrt{\beta\,/\,x}}{2\gamma x} \right) \text{Birnbaum-Saunders distribution} \tag{21}$$

Fitted distribution	Test statistic	Critical value		Test result	
		$\alpha = 0.05$	$\alpha = 0.01$	$\alpha = 0.05$	$\alpha = 0.01$
Birnbaum-Saunders	0.0941	0.1669	0.2003	Accept	Accept
Extreme Value	0.1482			Accept	Accept
Gamma	0.0881			Accept	Accept
Generalized Extreme Value	0.0997			Accept	Accept
Inverse Gaussian	0.0944			Accept	Accept
Log-logistic	0.1032			Accept	Accept
Logistic	0.1010			Accept	Accept
Lognormal	0.0937			Accept	Accept
Nakagami	0.0882			Accept	Accept
Normal (Gaussian)	0.1046			Accept	Accept

Table 8: Results of Kolmogorov-Smirnov goodness-of-fit test for DoB_{ch0} sample.

Fitted distribution	Test statistic	Critical value		Test result	
		$\alpha = 0.05$	$\alpha = 0.01$	$\alpha = 0.05$	$\alpha = 0.01$
Birnbaum-Saunders	0.0666	0.0501	0.0600	Reject	Reject
Extreme Value	0.1338			Reject	Reject
Gamma	0.0613			Reject	Reject
Generalized Extreme Value	0.0736			Reject	Reject
Inverse Gaussian	0.0666			Reject	Reject
Log-logistic	0.0561			Reject	Accept
Logistic	0.0637			Reject	Reject
Lognormal	0.0665			Reject	Reject
Nakagami	0.0657			Reject	Reject
Normal (Gaussian)	0.0707			Reject	Reject

Table 9: Results of Kolmogorov-Smirnov goodness-of-fit test for DoB_{ch45} sample.

Fitted distribution	Test statistic	Critical value		Test result	
		$\alpha = 0.05$	$\alpha = 0.01$	$\alpha = 0.05$	$\alpha = 0.01$
Birnbaum-Saunders	0.0557	0.0501	0.0600	Reject	Accept
Extreme Value	0.1190			Reject	Reject
Gamma	0.0645			Reject	Reject
Generalized Extreme Value	0.0596			Accept	Accept
Inverse Gaussian	0.0557			Reject	Accept
Log-logistic	0.0580			Reject	Accept
Logistic	0.0715			Reject	Reject
Lognormal	0.0558			Reject	Accept
Nakagami	0.0728			Reject	Reject
Normal (Gaussian)	0.0809			Reject	Reject

Table 10: Results of Kolmogorov-Smirnov goodness-of-fit test for DoB_{ch180} sample.

$$f_X(x) = \frac{1}{\sigma}\exp\left\{-\left(1+k\frac{x-\mu}{\sigma}\right)^{-1/k}\right\}\left(1+k\frac{x-\mu}{\sigma}\right)^{-1-\frac{1}{k}} \quad \text{Generalized Extreme Value distribution} \quad (22)$$

$$f_X(x) = \frac{\left(\beta \,/\, \alpha\right)\left(x \,/\, \alpha\right)^{\beta-1}}{\left(1+\left(x \,/\, \alpha\right)^{\beta}\right)^2} \quad \text{Log-logistic distribution} \tag{23}$$

where $\Gamma(a)$ is the Gamma function defined as follows:

$$\Gamma(a) = \int_0^{\infty} e^{-t} t^{a-1} dt \tag{24}$$

After substituting the values of estimated parameters from Table 3, following probability density functions are proposed for the crack shape factor (Y_c) and geometric factor (Y_g) in tubular K-joints under balanced axial loads, respectively.

$$\underset{Y_c}{f_X(x)} = (1.0019\times10^{-7})x^{37.39}e^{-x/0.110308} \tag{25}$$

$$\underset{Y_g}{f_X(x)} = \frac{1}{\sqrt{2\pi}}\exp\left\{-\frac{\left(\sqrt{x \,/\, 1.81261}-\sqrt{1.81261 \,/\, x}\right)^2}{0.85869}\right\}\left(\frac{\sqrt{x \,/\, 1.81261}+\sqrt{1.81261 \,/\, x}}{1.31049x}\right) \tag{26}$$

After substituting the values of estimated parameters from Table 4, following probability density functions are proposed for DoB_{ch}, DoB_{ch0}, DoB_{ch45}, and DoB_{ch180} in axially loaded tubular K-joints, respectively.

$$\underset{\mathrm{DoB_{ch}}}{f_X(x)} = \frac{1}{0.3750}\exp\left\{-\left(1+0.2564\frac{x-0.9064}{0.3750}\right)^{-3.8998}\right\}\left(1+0.2564\frac{x-0.9064}{0.3750}\right)^{-4.8998} \tag{27}$$

$$\underset{\mathrm{B_{ch0}}}{f_X(x)} = \left(2.2803\times10^{5}\right)x^{10.9476}e^{-x/0.08317} \tag{28}$$

$$\underset{\mathrm{B_{ch45}}}{f_X(x)} = \frac{0.27597\left(x \,/\, 0.2809\right)^{-0.9225}}{\left(1+\left(x \,/\, 0.2809\right)^{0.077527}\right)^2} \tag{29}$$

$$\underset{\mathrm{DoB_{ch180}}}{f_X(x)} = 0.3989\exp\left\{-\frac{\left(\sqrt{x \,/\, 0.78288}-\sqrt{0.78288 \,/\, x}\right)^2}{0.03855}\right\}\left(\frac{\sqrt{x \,/\, 0.78288}+\sqrt{0.78288 \,/\, x}}{0.27767x}\right) \tag{30}$$

These proposed PDFs, shown in Figures 12 and 13, can be adapted in the FM-based fatigue reliability analysis of axially loaded tubular K-joints which are commonly found in offshore jacket structures.

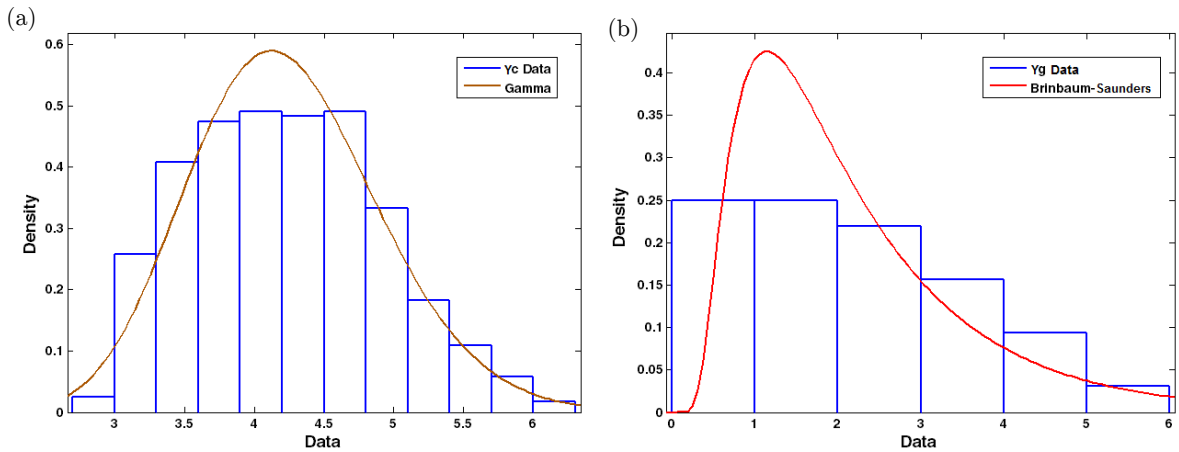


Figure 12: PDFs proposed for Y_c and Y_g:
(a) Crack shape factor Y_c – Gamma distribution, (b) Geometric factor Y_g – Birnbaum-Saunders distribution.

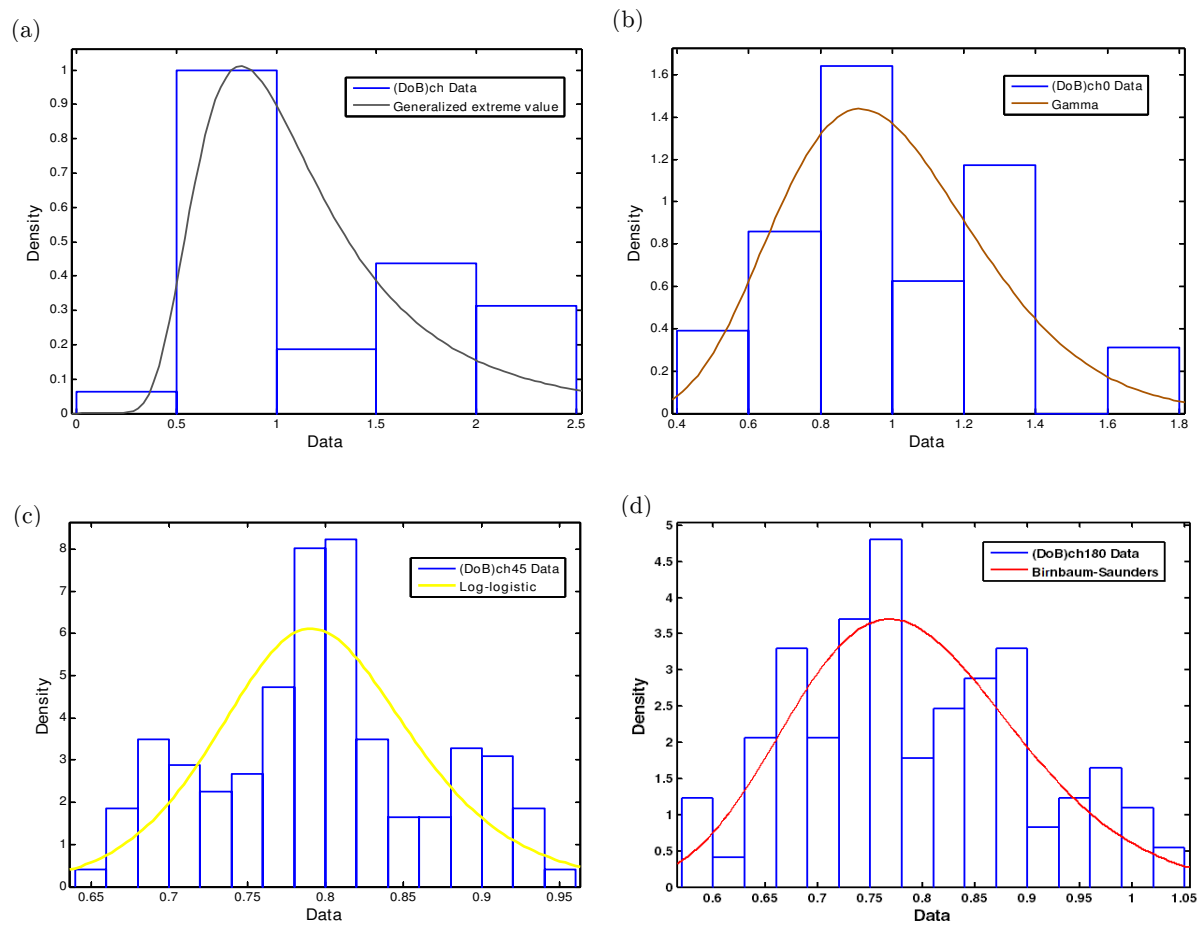


Figure 13: Proposed PDFs for the DoB:
(a) DoB_{ch} – Generalized extreme value distribution. (b) DoB_{ch0} – Gamma distribution.
(c) DoB_{ch45} – Log-logistic distribution. (d) DoB_{ch180} – Birnbaum-Saunders distribution.

9 CONCLUSIONS

In the present paper, results of parametric equations available for the computation of the DoB, Y_g, and Y_c were used to propose probability distribution models for these parameters in axially loaded tubular K-joints. Based on a parametric study, a set of samples were prepared for the DoB, Y_g, and Y_c; and the density histograms were generated for these samples using Freedman-Diaconis method. Ten different PDFs were fitted to these histograms. The ML method was used to determine the parameters of fitted distributions; and in each case, Kolmogorov-Smirnov test was utilized to evaluate the goodness of fit. It was concluded that Gamma and Birnbaum-Saunders distributions are the best probability models for Y_c and Y_g, respectively; and Generalized Extreme Value, Gamma, Log-logistic, and Birnbaum-Saunders distributions are the best probability models for DoB_{ch}, DoB_{ch0}, DoB_{ch45}, and DoB_{ch180}, respectively. Finally, after the substitution of estimated parameters, a set of fully defined PDFs were proposed which can be used in the FM-based fatigue reliability analysis of axially loaded tubular K-joints.

References

Ahmadi, H., Lotfollahi-Yaghin, M.A., Aminfar, M.H., (2011). Geometrical effect on SCF distribution in uni-planar tubular DKT-joints under axial loads. Journal of Constructional Steel Research 67: 1282–91.

Ahmadi, H., Lotfollahi-Yaghin, M.A., (2012). Geometrically parametric study of central brace SCFs in offshore three-planar tubular KT-joints. Journal of Constructional Steel Research 71: 149–61.

Ahmadi, H., Lotfollahi-Yaghin, M.A., Shao, Y.B., (2013). Chord-side SCF distribution of central brace in internally ring-stiffened tubular KT-joints: A geometrically parametric study. Thin-Walled Structures 70: 93—105.

American Petroleum Institute (API), (2007). Recommended practice for planning, designing and constructing fixed offshore platforms: Working stress design: RP2A-WSD. 21st Edition, Errata and Supplement 3, Washington DC, US.

Bowness, D., Lee, M.M.K., (1998). Fatigue crack curvature under the weld toe in an offshore tubular joint. International Journal of Fatigue 20(6): 481–90.

Chang, E., Dover, W.D., (1999). Parametric equations to predict stress distributions along the intersection of tubular X and DT-joints. International Journal of Fatigue 21: 619–35.

Connolly, M.P.M., (1986). A fracture mechanics approach to the fatigue assessment of tubular welded Y and K-joints. PhD Thesis, University College London, UK.

Efthymiou, M., (1988). Development of SCF formulae and generalized influence functions for use in fatigue analysis. OTJ 88, Surrey, UK.

Hellier, A.K., Connolly, M., Dover, W.D., (1990). Stress concentration factors for tubular Y and T-joints. International Journal of Fatigue 12: 13–23.

Kottegoda, N.T., Rosso, R., (2008). Applied statistics for civil and environmental engineers. 2nd Edition, Blackwell Publishing Ltd, UK.

Lee, C.K., Lie, S.T., Chiew, S.P., Shao, Y.B., (2005). Numerical models verification of cracked tubular T, Y and K-joints under combined loads. Engineering Fracture Mechanics 72: 983–1009.

Lotfollahi-Yaghin, M.A., Ahmadi, H., (2010). Effect of geometrical parameters on SCF distribution along the weld toe of tubular KT-joints under balanced axial loads. International Journal of Fatigue 32: 703–19.

Lotfollahi-Yaghin, M.A., Ahmadi, H., (2011). Geometric stress distribution along the weld toe of the outer brace in two-planar tubular DKT-joints: parametric study and deriving the SCF design equations. Marine Structures 24: 239–60.

Mohammadzadeh, S., Ahadi, S., Nouri, M., (2014). Stress-based fatigue reliability analysis of the rail fastening spring clip under traffic loads. Latin American Journal of Solids and Strucutres 11(6): 993-1011.

Morgan, M.R., Lee, M.M.K., (1998a). Parametric equations for distributions of stress concentration factors in tubular K-joints under out-of-plane moment loading. International Journal of Fatigue 20: 449–61.

Morgan, M.R., Lee, M.M.K., (1998b). Prediction of stress concentrations and degrees of bending in axially loaded tubular K-joints. Journal of Constructional Steel Research 45(1): 67–97.

Shao, Y.B., (2006). Analysis of stress intensity factor (SIF) for cracked tubular K-joints subjected to balanced axial load. Engineering Failure Analysis 13: 44–64.

Shao, Y.B., (2007). Geometrical effect on the stress distribution along weld toe for tubular T- and K-joints under axial loading. Journal of Constructional Steel Research 63: 1351–60.

Shao, Y.B., Du, Z.F., Lie, S.T., (2009). Prediction of hot spot stress distribution for tubular K-joints under basic loadings. Journal of Constructional Steel Research 65: 2011–26.

Shao, Y.B., Lie, S.T., (2005). Parametric equation of stress intensity factor for tubular K-joint under balanced axial loads. International Journal of Fatigue 27: 666–79.

Wordsworth, A.C., Smedley, G.P., (1978). Stress concentrations at unstiffened tubular joints. Proceedings of the European Offshore Steels Research Seminar, Paper 31, Cambridge, UK.